J2.1 **WAVE FLOW SIMULATIONS OVER ARCTIC LEADS**

Thorsten Mauritsen*, Gunilla Svensson
Stockholm University, Stockholm, Sweden

Branko Grisogono
Department of Geophysics, Faculty of Science, Zagreb, Croatia

1. INTRODUCTION

The Arctic Ocean is covered with ice throughout the year. The average ice thickness varies with season around a few meters. However, due to the divergence of the upper ocean currents and the stress excerted on the ice surface by winds, both ridges with thicker ice and cracks with open water or thin ice, called leads, appear throughout the year (Lindsay and Rothrock, 1995; Miles and Barry, 1998). The leads introduce surface heteorogeneities, which affect the overlying atmosphere. A satellite image from an occasion of cloud free conditions is shown in Figure 1.

The leads are revealed to bee long and narrow, with a typical width of a few kilometers or less. The ice surface temperature may vary substantially throughout the year. During the Arctic summer, the ice surface temperature is usually close to the melting point. Shorter events of slightly colder surface temperatures occur throughout this period. During winter time the ice surface temperature can be below 40 ºC.

Large eddy simulations have been used to tackle the problem of stimating the heat fl from leads under idealize conditions. For instance, Zulauf and Krueger (2003) used a wide range of lead widths, different cross-wind speeds and winter-like conditions, to estimate both the heat flux and plume penetration height. The numerical experiments were performed with a temperature difference between the ice surface and the open lead of 27K.

It is well known that orographic obstacles can be a source of atmospheric gravity waves (Queney, 1948; Smith, 1979). These can have a wide range of effects such as wave-drag, clear air turbulence, hydraulic jumps etc (e.g. Grisogono, 1995). Moreover, gravity waves can transport momentum and energy far away from their sources (e.g. Nappo, 2002). It was also pointed out by Malkus and Stern (1953) that a at island, which is warmer than the surrounding sea, can be a source of internal gravity waves. It is, however, usually neglected that surface heteorogeneities of temperature and roughness can be sources of atmospheric gravity waves, even in the absence of orography.

It is the goal of this study to show that Arctic leads can be a source of standing gravity waves. Subsequently we give an insight into the complexities that may arise when these waves interact with the stable boundary layer. Further details and discussion can be found in Mauritsen et al. (2004).

* Corresponding address: Thorsten Mauritson, Department of Meteorology, Stockholm University, S-106 91 Stockholm, Sweden; e-mail: thorsten@misu.su.se

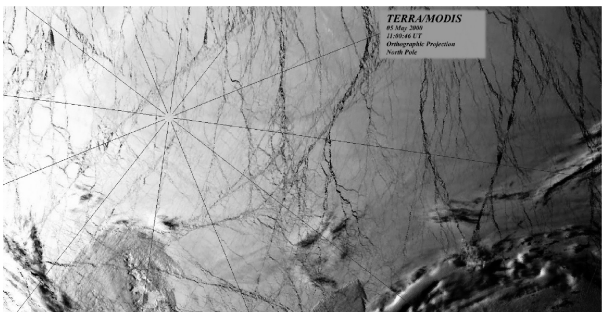

Figure 1. In this satellite image, the sea ice appears white and areas of open water, or recently refrozen sea surface, appear black. Note a considerable number of leads appearing as dark networks of lines. The irregular shapes in the lower part of the image are clouds. The image was acquired by the Moderate resolution Imaging Spectroradiometer (MODIS), on May 5, 2000. The image resolution is 1 km.

2. MODEL SETUP

The numerical model used in the present study was the atmospheric part of the Coupled Ocean/-Atmosphere Mesoscale Prediction System (COAMPS^{TM}) of version 2.0 (Hodur, 1997). The model domain was chosen to be two dimensional with periodic lateral boundary conditions. In the horizontal direction 600 gridpoints were used with a resolution of 500 m. Such high horizontal resolution can be applied because the model is non-hydrostatic. In the vertical, a total of 99 levels were used. Dense vertical resolution, with levels at 2, 6, 10, 16, 24 m etc., was used in and near the boundary layer with a transition to a constant vertical resolution of 150 m in the free troposphere. The model top was at 13 km. The roughness length was 0.01 m for the ice surface and variable about $5x10^{-5}$ m for the ocean. Moist and radiative processes along with Coriolis effects were neglected, even though we believe that these processes are important for the Arctic boundary layer. An ice lead was placed in the middle of the two-dimensional model domain. The ice surface was kept at constant temperature. The sea surface temperature was

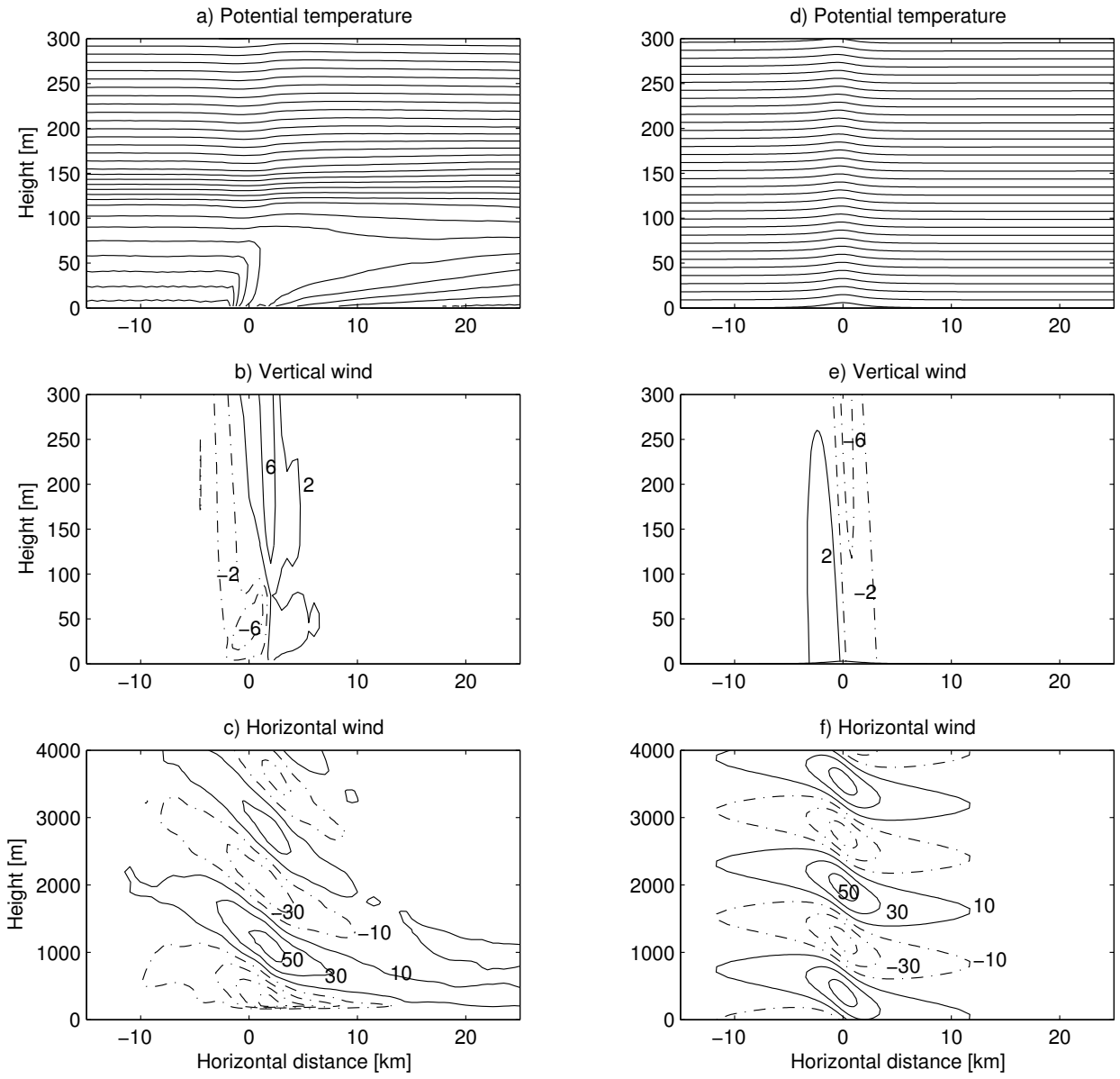

Figure 2. Results at 9h simulation time of the summertime lead (a-c) and analytical solution for flow over a small ridge (d-f). Upper panels show the boundary layer potential temperatures with a contour interval of 0.1 K. Middle panels show the vertical wind with contour intervals of 0.004 m s^{-1}, solid and dotted curves represent positive and negative anomalies, respectively. Lower panels show the free tropospheric horizontal wind deviation from mean with a contour interval of 0.02 m s^{-1}. The lead is at x = 0 and the wind is from left to right. Note the different vertical scales.

chosen to be at the freezing point of salt water. 7 grid points in the middle of the domain were defined to be sea surface: i.e. an effective width of the lead of 3 km. The initial atmospheric stratification was chosen to be constant throughout with a buoyancy frequency (N) of 0.02 s^{-1}.

3. RESULTS

Three simulations are presented. The first case represents conditions found during summer (temperature difference between sea and ice of 3K) and the other two are winter cases with strong temperature difference (27K) and with different background windspeed (5 and 2.5 ms^{-1}). The summer case was run with a background wind of 5 ms^{-1}.

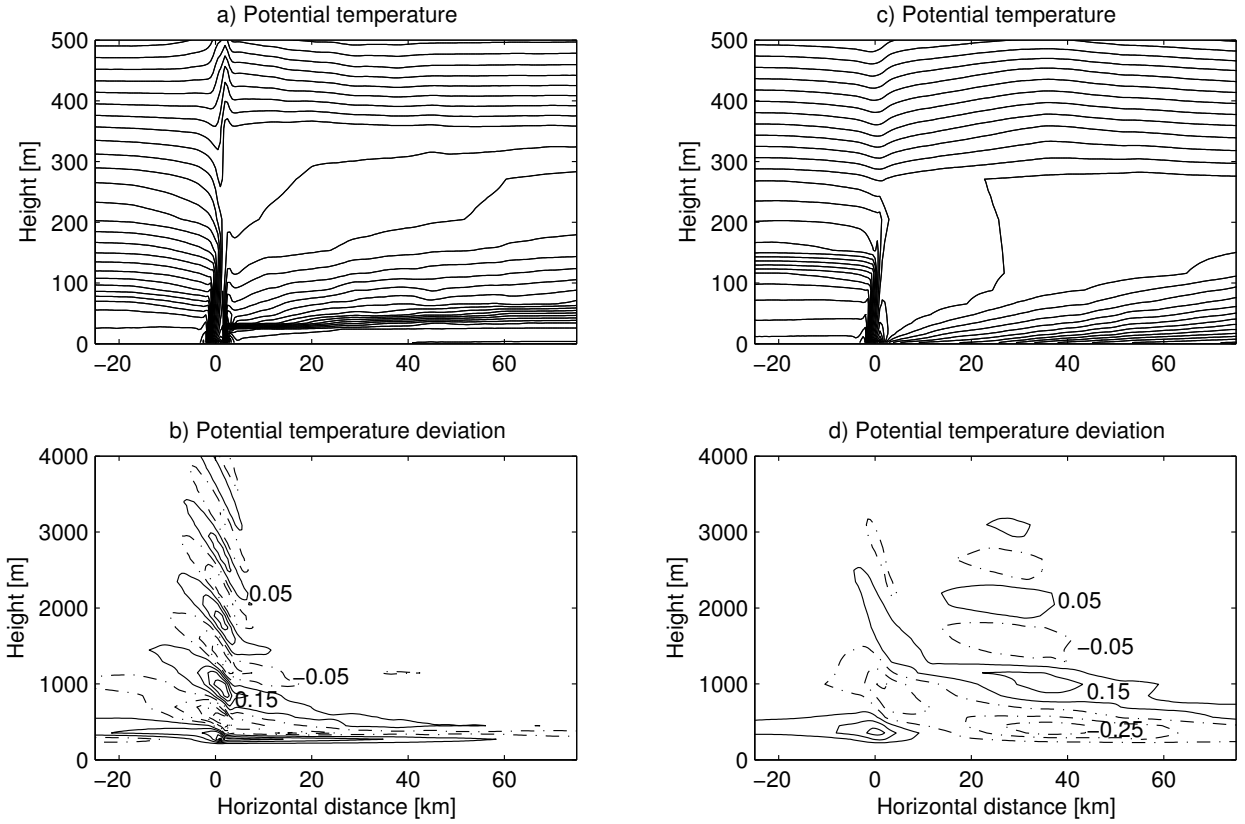

Figure 3. Results of two simulations with 27 K temperature difference between the lead and the ice surface after 12 hours of integration. In one case a-b U=2.5 ms^{-1}, whereas in the other case c-d U=5 ms^{-1}. In a and c the boundary layer potential temperature is shown with a contour interval of 0.2 K and in b and d the free troposphere potential temperature deviation from the mean is shown with a contour interval of 0.1 K. Dash dotted are negative values. Note also the variable vertical scales.

3.1 *Summer case*

The results of the summer case simulation are shown in Figure 2 a-c. Here a stably stratified boundary layer is formed upstream of the lead. An elevated inversion between 120 m and 160 m capping a turbulent layer of decreased stratification appears. A convective internal boundary layer extending up to approximately 80 m forms above the open lead (Figure 2a). This results in vertical mixing of heat and momentum. The convective mixing increases the average wind speed in the boundary layer above the lead. Due to continuity, there has to be downward vertical wind above the lead (Figure 2b). Downstream, a stable internal boundary layer develops. This results in a decreased average wind speed in the boundary layer, and a light positive vertical wind. A weak standing wave appears in the free troposphere (Figure 2c). The horizontal wind component of the wave has an amplitude of 0.05-0.10 ms^{-1}. Compared with the background wind of 5 ms^{-1} this indicates that linear wave theory is applicable. The horizontal wavelength is seen to be approximately 12 km, which is about four times the effective width of the lead and the ridge. For constant background wind and stratification the Taylor-Goldstein equation for standing gravity waves reads (e.g. Nappo, 2002):

$$\frac{d^2\hat{w}}{dz^2}+\left[\frac{N^2}{U^2}-k^2\right]\hat{w}=0$$

where $\hat{w}$ is the vertical wind amplitude, U is the background windspeed and k is the horizontal wavenumber. The term in the brackets can be considered as the square of a vertical wavenumber, m. Using the horizontal wavelength to find $k=2\pi/L_x$ gives a vertical wavelength $L_z=2\pi/m$ of 1580 m. This is close to the 1.6 km as found in the simulations (Figure 2 c).

We can compare the results of the simulation with an analytical solution of flow over a bell-shaped ridge. A solution has been found by Queney (1948) for the linearized two dimensional, hydrostatic, non-rotating, steady state flow equations using the Buossinesq approximation. This is a good approximation as long as the free flow Froude number is much larger than unity. The results are shown in Figure 2d-f for a ridge of height 3 km. The standing gravity wave found in the free troposphere is quite similar to the wave in the summer lead

case. However, there are some differences. Most pronounced is the 180-degree phase-shift of the wave (Figures 2c and 2f). This is because the mechanism for generating the wave is basically different. In the orographic wave case, the air is displaced upward by the ridge, leading to the positive low-level vertical wind on the upwind side and the negative vertical wind on the downwind side of the ridge simply due to continuity and the pressure distribution (Figure 2e). In the lead case on the contrary, the convective internal boundary layer causes more effective downward transport of momentum increasing the horizontal wind locally in the boundary layer. This leads to the downward wind on the upwind side and the upward wind on the downwind side seen in Figure 2b. Therefore, the wave is phase-shifted 180 degrees compared with the orographic wave case.

3.2 *Winter case*

During winter, there is often a substantial temperature difference between the lead and the ice-surface. When simulating this, atmospheric conditions were chosen close to those used in Zulauf and Krueger (2003), and surface temperature difference of 27 K. This is well within the range of observed wintertime surface temper

atures of the Arctic Ocean (Persson et al. 2002). The results of the two simulations are shown in Figure 3. A background stable boundary layer exists upstream of the lead. In both cases, convection rapidly heats the air above the lead, penetrating the background boundary layer inversion up to 250-350 m. For large eddy simulations, with the same background conditions, Zulauf and Krueger (2003) found a penetration height of 270 metres, which is practically the same as we found with the meso-scale model.

The difference in the boundary layer structure results in a distinct difference in the wave pattern found in the free troposphere (Figure 3 b and d). In both cases the primary wave appears above the lead, however, only the moderate wind case exhibits a secondary wave. This is probably because of the lack of a developing stably stratified internal boundary layer in the weak wind case. The secondary wave extends approximately 50 km downstream of the lead. It appears to have a wavelength on the order of 100 km, which is nearly two orders of magnitude more than the width of the lead itself. We find a vertical wavelength Lz = 0:8 km in Figure 3 b and twice of that in 2 d, which is expected. The wave amplitudes are more than an order of magnitude stronger than in the summer case. The presence of the lead affects the vertical structure of TKE far downstream of the lead.

We inspect the temporal evolution of TKE downstream of the lead in Figure 5. After a few hours the two-layer structure of TKE appears, which remains for the entire simulation. While the lower shear driven layer reaches steady-state after about 7 hours, the upper convective layer is found to be intermittent throughout the simulation. This behaviour somewhat resembles the quasi-propagating hydraulic jump, found in Enger and Grisogono (1998) Note that the high levels of TKE during the first hour of the simulation is partly artificial due to the model spinup.

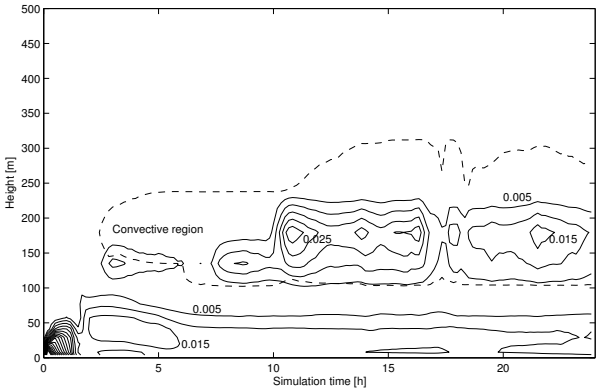

Figure 4. Time evolution of turbulent kinetic energy in the boundary layer 25 km downstream of the lead for the 5 ms^{-1} background wind case. Solid contour every 5 $x10^{-3}$ m^2 s^{-2}. The dashed line indicates convective instability.

4. CONCLUSION

We have shown that Arctic leads can be a source of standing atmospheric gravity waves. In the first case, we considered conditions representative of the summertime Arctic. The temperature difference between the ice and lead surface was set to 3K and the atmosphere was stably stratified throughout. A standing linear gravity wave appeared above the lead. The wave flow over the lead was found to be similar to the flow over a small ridge. It is important to note that this is only possible for the long-lived stable boundary layer. The mid-latitude nocturnal boundary layer is usually capped by a near-neutral residual layer, which prevents internal gravity wave propagation.

In two exploratory simulations with conditions typical of the wintertime Arctic, the wave may interact with the stable boundary layer. In a weak-wind case, the convection dominated over the background wind generating a secondary circulation, which reversed downstream surface winds. This caused an elevated layer of turbulence due to shear. In the second, moderate-wind case wave-breaking caused convective instabilities in an elevated layer up to 50 km downstream of the lead. The wave-breaking turbulence was found to be intermittent.

REFERENCES

Enger, L. and B. Grisogono, 1998: The response of bora-type flow to sea surface temperature. *Quart. J. Roy. Meteorol. Soc.,* **124**, 1227-1244.

Grisogono, B., 1995: Wave drag effects in a mesoscale model with higher-order closure turbulence scheme. *J. Appl. Meteorol.,* **34**, 941-954.

Hodur, R. M.,1997: The Naval Research Laboratory's Coupled Ocean/Atmosphere Mesoscale Prediction System (COAMPS™). *Mon. Wea. Rev.,* **125**, 1414-1430.

Lindsay, R. W. and D. A. Rothrock, 1995: Arctic sea ice leads from advanced very high resolution radiometer images. *J. Geophys. Res.,* **100**, 4533-4544.

Malkus, J. S. and M. E. Stern, 1953: The ow of a stable atmosphere over a heated island, part I. *J. Meteorol.*, **10**, 30-41.

Mauritson, T., G. Svensson and B. Grisogono, 2004: Wave flow simulations over Arctic leads. *Submitted to Bound-Layer Meteor.*

Miles, M. W. and R. G. Barry, 1998: A 5-year satellite climatology of winter sea ice leads in the western Arctic. *J. Geophys. Res.,* **103**, 21723-21734.

Nappo, C. J., 2002: *An introduction to Atmospheric Gravity Waves.* International geophysics series. Volume 85. Academic Press, 276 pp.

Persson, P. O. G., C. W. Fairall, E. L. Andreas, P. S. Guest, and D. K. Perovich, 2002: Measurements near the Atmospheric Surface Flux Group tower at SHEBA: Near-surface conditions and surface energy budget. *J. Geophys. Res.*, **107**, 8045, doi:10.1029/2000JC000705.

Queney, P., 1948: The problem of air flow over mountains: A summary of theoretical studies. *Bull. Amer. Meteorol. Soc.,* **29**, 16-26.

Smith, R. B., 1979: Influence of mountains on the atmosphere. *Adv. Geophys.*, **21**, 87-217.

Zulauf, M. A. and S. K. Krueger, 2003: Two-dimensional numerical simulations of Arctic leads: Plume penetration height. *J. Geophys. Res.,* **108**.